IMMUNOBIOLOGY

Role of the monoclonal κ chain V domain and reversibility of renal damage in a transgenic model of acquired Fanconi syndrome

Christophe Sirac, Frank Bridoux, Claire Carrion, Olivier Devuyst, Béatrice Fernandez, Jean-Michel Goujon, Chahrazed El Hamel, Jean-Claude Aldigier, Guy Touchard, and Michel Cogné

Acquired Fanconi syndrome (FS) is a complication of monoclonal gammopathies featuring a generalized dysfunction of the proximal tubule of the kidney, due to the storage within proximal tubular cells of a monoclonal immunoglobulin light chain. We engineered transgenic mice in which the endogenous mouse Jκ cluster was replaced by a human VκJκ rearranged gene cloned from a patient with smoldering myeloma-associated FS. The V region belonged to the VκI subgroup and was related to the *O2-O12* germ-line gene, a V segment previously found associated with FS and light-chain crystallization in several patients with myeloma. Association of the human VκI domain with a mouse κ constant domain in transgenic animals yielded a nephrotoxicity pattern similar to that observed in patients, strongly suggesting that the whole pathogenic effect of FS light chains can be ascribed to a peculiar structure of the V domain. Morphologic alterations of the kidney tubular cells, which contained rhomboid-shape crystals, were observed in mice, together with alterations of the proximal tubule reabsorption function. Moreover, the number of renal crystalline inclusions was dramatically reduced after conditional deletion of the human VκI transgene, showing that proximal tubular lesions are reversible upon suppression of the nephrotoxic light chain secretion. (Blood. 2006;108:536-543)

© 2006 by The American Society of Hematology

Introduction

Production of a free monoclonal immunoglobulin (Ig) light chain (LC) by malignant plasma cells may be responsible for severe complications. Tissue deposition may occur in the form of amyloid light-chain deposits (AL-amyloidosis) or of nonamyloid LC deposition disease (LCDD), 2 systemic diseases with renal manifestations characterized by predominant glomerular symptoms. Renal alterations resulting from specific tubular involvement, myeloma cast nephropathy, and Fanconi syndrome (FS) are also a frequent outcome.[1,2] Myeloma cast nephropathy (MCN) is a common complication of high-mass myeloma, in which casts made up of Tamm-Horsfall protein and monoclonal LC obstruct distal tubule lumens, leading to acute renal failure.[3,4] FS is a rare entity, characterized by a generalized dysfunction of the epithelial cells lining the proximal tubule, leading to low-molecular-weight proteinuria, generalized aminoaciduria, glycosuria, phosphaturia, uricosuria, and proximal (type II) renal tubular acidosis.[5] Typically, LC-associated FS occurs in smoldering myeloma patients with associated production and urinary secretion of a monoclonal LC, almost always of κ type. Most of the reported cases of FS feature the presence of κ LC crystalline inclusions within the endolysosomal compartment of proximal tubular cells. Crystalline inclusions also are detected commonly in the cytoplasm of macrophages and

malignant plasma cells and may be involved in the slow progression of the plasma-cell disorder.[5]

We previously studied and sequenced at the cDNA level the monoclonal κ LC *CHEB* involved in FS.[6] Small protein–enriched gel filtration fractions from the patient's urine yielded crystals morphologically similar to those found in the patient's proximal tubular cells, with the same 80-Å periodicity on electron micrographs. The crystals contained a 107–amino acid fragment (with a C-terminal lysine) corresponding to the variable (V) domain together with a low proportion of the entire κ chain. In vitro trypsin, pepsin, or cathepsin B treatment of the native entire κ LC yielded a homogeneous V domain fragment which, in contrast to other monoclonal κ LCs, was completely resistant to further proteolytic digest.[7,8] The patient's κ chain also displayed an unusual self-reactivity by Western blotting. Genes encoding *CHEB* as well as all other VκI LCs from patients with FS featuring intracellular crystals were shown to derive from the same germ-line gene *O2/O12* or to another closely related VκI germ-line gene, *O8/O18*.[5,8-10] To date, the cellular mechanisms by which monoclonal κ LCs induce proximal tubular dysfunction remain poorly understood.

Among the broad spectrum of Ig deposition diseases, a number of human monoclonal LCs responsible for tissue deposits have now been studied at the molecular level.[11-26] However, few in vivo

experimental models are available and none allowed complete studies of renal physiologic disturbances or therapeutic approaches. We previously developed models in which transfected hybridoma cells expressing a human LC were grafted to mice. These models featured renal lesions similar to those observed in the patient from whom the monoclonal LC sequence was cloned (ie, either LCDD [involving κ LC FRA][27] or FS [involving κ LC CHEB]).[28] In the latter model, we showed that limited sequence changes of the V region determined the development of proximal tubular lesions. Unfortunately, in vivo studies of proximal tubule function could not be performed in these animals due to their poor general condition and short survival related to the rapid tumor growth. To overcome this problem and to more specifically assess the role of the V domain in the tissue deposition process, we have generated a transgenic model by targeted insertion of the rearranged VκJκ gene *CHEB* in the κ locus. These mice express a hybrid κ Ig LC comprising the human V domain and the mouse C region. Despite the replacement of the human C region, animals exhibit proximal tubular lesions typical of FS with LC crystals, which is consistent with the fact that LC aggregation is promoted by the V domain structure. We show that the extent of tubular inclusions is proportional to the serum production rate of CHEB LCs and that renal lesions may recover after conditional deletion of the human VκI transgene. Moreover, these mice display the major phenotypic characteristics of FS and thus provide the first complete experimental model for a monoclonal LC-associated renal disease.

Materials and methods

Gene targeting

A 12.7-kb *Bam*HI genomic fragment corresponding to the germ-line mouse JκCκ cluster was used to generate the VκJκ *CHEB* targeting construct. A 2.2-kb *Bsm*I/*Sac*I fragment containing the 5 Jκ segments was replaced with a "κ-*Neo*" cassette including a LoxP flanked neomycin resistance gene (*Neo^R*), the rearranged VκJκ *CHEB,* and a third LoxP site downstream of the VκJκ *CHEB* gene. The resulting 3 lox-P sites were in the same orientation allowing Cre-mediated deletion of either the *Neo^R* gene alone (κ-CHEB mice) or both the *Neo^R* gene and the VκJκ *CHEB* gene (κ-del mice) (Figure 1). Cells of the embryonic stem (ES) cell line E14 were transfected with the linearized vector by electroporation and selected using G418 (400 μg/mL). Southern blot analysis of a *Bam*HI restriction with an external 3′ probe (Cκ probe, a 1.6-kb Afl2 genomic fragment) identified recombinants, yielding a 4.5-kb *Bam*HI band in place of the 12.7-kb *Bam*HI band for the wild-type (*wt*) allele. Two positive ES-cell clones were injected into C57BL/6 blastocysts, and the resulting male chimeras were mated with C57BL/6 females. Germ-line transmission in mutant mice was assessed by coat color, and the presence of the homologous recombination at the Igκ locus was checked by Southern blot and polymerase chain reaction (PCR). These "κ-*Neo*" mice were mated with EIIa-Cre transgenic mice (a gift from Dr Westphal, used under a noncommercial research license agreement from DuPont, Wilmington, DE), in order to yield the κ-CHEB and κ-del mutant mice. The resulting progeny were checked by Southern blot either for the *Neo^R* gene deletion only (κ-CHEB mice), preserving the 4.5-kb *Bam*HI Cκ-hybridizing band, or for the *Neo^R* plus VκJκ *CHEB* joint deletion (κ-del mice) yielding a 10.5-kb band, while both types of Cre-mediated deletions resulted in a loss of the 5′Jκ/*Neo* amplification by PCR. As a VκJκ *CHEB* gene deletion only was not distinguishable from the *wt* allele by Southern blot (both yielding an approximately 12.7-kb *Bam*HI band), we used only the 5′Jκ/*Neo* PCR to check this event. 5′Jκ/*Neo* PCR (35 cycles at 55°C) was done using 5′Jκ primer (5′CCAC-CATCTAGCCCAGGAAAAGTTACA3′) and Neo3 primer (5′CT-TGACGAGTTCTTCTGAGGGGATCGGCA3′).
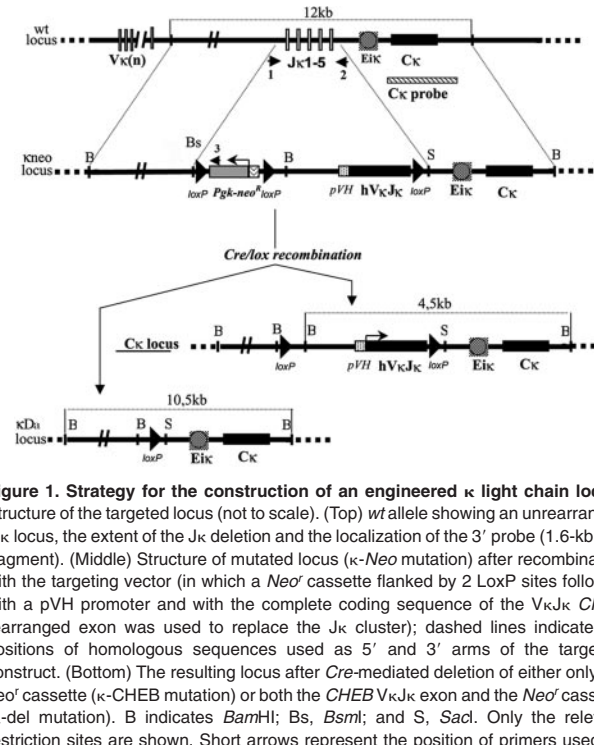
Figure 1. Strategy for the construction of an engineered κ light chain locus. Structure of the targeted locus (not to scale). (Top) *wt* allele showing an unrearranged Igκ locus, the extent of the Jκ deletion and the localization of the 3′ probe (1.6-kb Afl2 fragment). (Middle) Structure of mutated locus (κ-*Neo* mutation) after recombination with the targeting vector (in which a *Neo^r* cassette flanked by 2 LoxP sites followed with a pVH promoter and with the complete coding sequence of the VκJκ *CHEB* rearranged exon was used to replace the Jκ cluster); dashed lines indicate the positions of homologous sequences used as 5′ and 3′ arms of the targeting construct. (Bottom) The resulting locus after *Cre*-mediated deletion of either only the neo^r cassette (κ-CHEB mutation) or both the *CHEB* VκJκ exon and the *Neo^r* cassette (κ-del mutation). B indicates *Bam*HI; Bs, *Bsm*I; and S, *Sac*I. Only the relevant restriction sites are shown. Short arrows represent the position of primers used for PCR as described in "Materials and methods." 1 indicates 5′Jκ; 2, 3′Jκ; and 3, Neo3.

Flow cytometric analysis

Single-cell suspensions from spleen and bone marrow were washed in RPMI medium supplemented with 10% fetal calf serum (FCS)/2% rabbit serum (to avoid Fc receptor staining with rat antibodies), and stained (5×10^5 cells per assay) with appropriate antibodies. Data were collected on a COULTER XL flow cytometer (Beckman Coulter, Brea, CA), and analyzed using WinMDI software (The Scripps Research Institute, La Jolla, CA). Rat anti–mouse B220-PC5 was purchased from Southern Biotechnologies Associates (Birmingham, AL). Goat anti–mouse κ chains (Southern Biotechnologies Associates) was labeled using Alexa 488 (Molecular Probes, Eugene, OR), and was used to specifically recognize the murine Cκ domain of the hybrid CHEB LC.

ELISA assays

Sera and urines from homozygous κ-Neo, homozygous κ-CHEB, heterozygous κ-CHEB/κ-del, homozygous κ-del mutant mice, and normal littermates were analyzed for the presence of κ light chains. Enzyme-linked immunosorbent assays (ELISAs) were performed in polycarbonate 96-multiwell plates (Maxisorb; Nunc, Roskilde, Denmark), coated overnight at 4°C (100 μL/well) with 2 μg/mL of goat anti–mouse κ chains (Southern Biotech Associates) diluted in 0.05 M sodium bicarbonate buffer. After blocking with 1% bovine serum albumin/phosphate-buffered saline (BSA/PBS) buffer and washing steps in 0.1% Tween 20/PBS buffer, 100 μL serum (first diluted to 1:200), urine (first diluted to 1:10) or mouse standard κ LC (Southern Biotechnologies Associates) were diluted into successive wells in 1% BSA/PBS buffer and incubated for 2 hours at 37°C. After washing, 100 μL/well of alkaline phosphatase–conjugated goat anti–κ (1 μg/mL; Southern Biotechnologies Associates), diluted in 0.1% Tween 20/PBS buffer, was added and adsorbed in 1.5 hours at 37°C. After washing, phosphatase alkaline activity was assayed on 1 mg/mL alkaline phosphatase substrate (Sigma-Aldrich, St Louis, MO) and blocked with addition of 50 μL/well of 3 M NaOH. Optical density was measured at 420 nm in a Spectracount photometer (Packard, Meriden, CT).

Nucleic acid studies and sequence analysis

Total RNA (10 μg) was analyzed on 1% agarose and 0.7 M formaldehyde gels, transferred onto nylon sheets (Amersham, Buckinghamshire, United

Kingdom), and hybridized with a mouse κ probe corresponding to the 1.6-kb Afl2 genomic fragment including the entire Cκ exon.

Total RNA from splenocytes (2 μg) were used as templates for synthesis of single-stranded cDNA by reverse transcriptase (Boerhinger, Mannheim, Germany). cDNA were amplified by PCR,[29] cloned and sequenced by the dideoxynucleotide termination method[30] using T7 polymerase and an automated laser fluorescent ABI 3100 DNA sequencer (Perkin-Elmer, Branchburg, NJ).

Induction of VκJκ *CHEB* Cre deletion

κ-CHEB mice were mated with Mx-Cre mice (a kind gift from Prof K. Rajewsky, Harvard Medical School, Boston, MA) that carried the Cre gene under the control of a type I interferon-inducible promoter Mx1.[31] The progeny was controlled by Southern blotting to assess the presence of the Mx-Cre transgene and the κ-CHEB knock-in transgene. Mice were also checked for the absence of the E2A-Cre transgene.

Double transgenic κ-CHEB/Mx-Cre mice were intraperitoneally injected with pI-pC (400 μg), a synthetic double-strain RNA which induces type I interferon (IFNα/β) production. pI-pC injections (200 μg) were repeated weekly during the first month. Completion of the *Cre*-mediated conditional deletion was checked at the sacrifice of mice by fluorescence-activated cell-sorting (FACS) analysis of splenocytes LC expression and occasionally checked by PCR (32 cycles at 52°C) using 5′Jκ primer and 3′Jκ primer (5′TGTTCTCTTCAGATTAGTG3′) (Figure 1).

Animal preparations

Mice (2 to 6 months old) were used for flow cytometric analysis and pathologic and metabolic studies. They were maintained under conventional conditions in our animal facility, following principles of laboratory animal care. Organs were obtained after killing with carbon dioxide, according to recommendations of the local ethics committee. In some experiments, unilateral nephrectomy was performed under anesthesia in 1-month-old double transgenic κ-CHEB/κ-del/Mx-Cre mice prior to deletion of the *κ-CHEB* knock-in gene, as previously described.[32] Metabolic studies were conducted on female age-matched wt, homozygous κ-CHEB, or heterozygous κ-CHEB/κ-del mice, placed in metabolic cages with ad libitum access to normal food and water (Lab Diet-PMI Nutrition International, Elkridge, MD). Biochemical parameters were measured on 24-hour urine collections, and simultaneous blood samples were obtained by retro-orbital puncture under anesthesia.

Immunomorphologic analysis

Kidney samples were processed for light microscopic examination, immunofluorescence, and electron microscopic studies, as previously described.[28] Histologic sections were mounted with Pertex medium (Histolab, Gothenburg, Sweden) for light microscopy using a Zeiss Axioplan microscope equipped with Plan Neufluar 20 ×/0.5, 40 ×/0.75, and 100 ×/1.3 objective lenses (Carl Zeiss, Le Pecq, France). Images were acquired through an Olympus C-5060 camera and processed using Quick Photo Pro MIS version 1.2 software (Olympus Europa, Hamburg, Germany). Immunohistochemistry was performed on paraffin-embedded sections, using the UltraVision Detection System (Lab Vision, Newmarket, United Kingdom) with a mouse monoclonal antibody against human κ or λ LC (Novocastra, Newcastle Upon Tyne, United Kingdom) and with a rabbit polyclonal anti–mouse cathepsin B (Upstate, Lake Placid, NY), according to manufacturer's protocol. For ultrastructural examination, kidney samples were fixed with 4% glutaraldehyde in PBS (pH 7.4) at 4°C for 2 hours. After washing with 0.1 M PBS, samples were post-fixed with 1% osmium tetroxide, dehydrated, and embedded in araldite. Ultrathin sections were examined with a JEOL 1010 transmission electron microscope (JEOL, Tokyo, Japan) after uranyl acetate and lead citrate staining.

The extent of proximal tubule crystalline inclusions was assessed by counting the maximal number of crystals by proximal tubule section detected by light microscopic examination of toluidine blue–stained semithin sections after araldite inclusion. All proximal tubule sections present on the kidney sample were examined. The score of crystal formation was graded from 0 to 4, as follows: 0 represents no detectable crystal (confirmed in each case by electron microscopy), while 2+, 3+, and 4+ represent 1 to 2, 3 to 5, 6 to 10, and more than 10 crystals per tubule section.

Urine and plasma analyses

Urine concentrations of Clara-cell protein (CC16), a 16-kDa marker for early detection of proximal tubule dysfunction, were measured as previously described.[33,34] Serum and urinary electrolytes and creatinine and urine amino acids were measured by standard methods.[34] Fractional excretions (FEs) of uric acid and phosphate were calculated as follows:

FE {X} (%) = Urine {X} concentration × serum creatinine concentration × 100; Serum {X} concentration × urine creatinine concentration.

Statistical analysis

Data are expressed as means plus or minus SD. Comparisons between the different groups of mice were assessed by using unpaired Student t test or 1-way factorial analysis of variance (ANOVA) with Bonferroni or Tukey Kramer correction when appropriate. P values less than .05 were considered statistically significant.
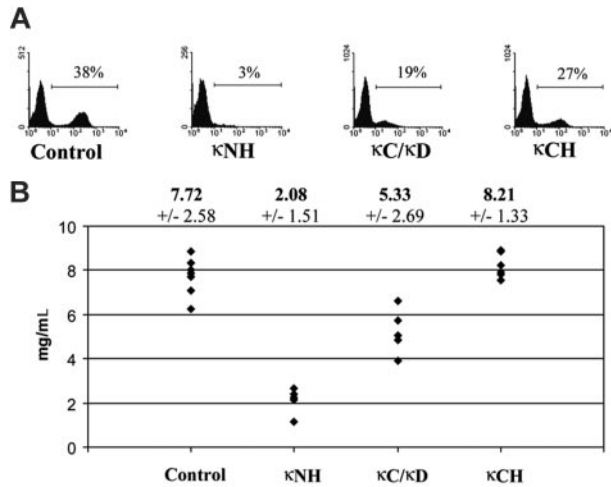
Results

Efficient production of chimeric κ-CHEB LC in transgenic mice

Efficient production of a chimeric LC, made up of a V domain of human origin (encoded by the knock-in *CHEB* VκJκ exon) and of a mouse C domain, was observed in transgenic mice. We first checked the identity of LC produced in mice with the product that could be predicted from the knock-in experiment design. Northern blotting of total RNAs from splenocytes showed normal-sized κ mRNAs that hybridized both with a murine Cκ probe and with the *CHEB* V exon probe (data not shown). The absence of any mutation in the knock-in exon and its correct splicing to the endogenous Cκ was checked by sequencing κ cDNAs from κ-CHEB mouse splenocytes.
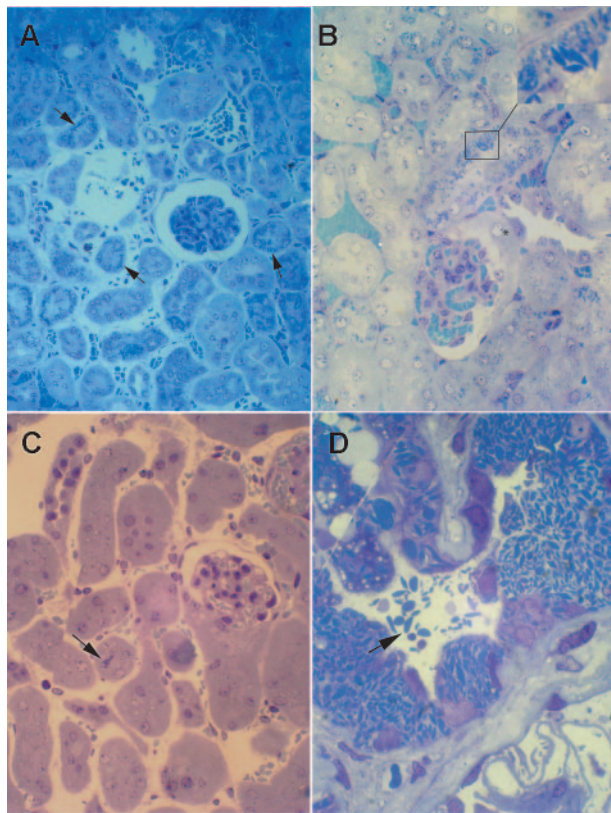
Expression of κ LC was low in mice still carrying the *CHEB* V gene flanked with the *neo^r* cassette used for ES clone selection in vitro. Expression was more efficient after *Cre*-deletion of the *neo* cassette in heterozygous κ-CHEB/κ-del, and was still higher in homozygous κ-CHEB mice as seen by flow cytometric analysis (Figure 2A). κ LC serum rates were checked by ELISAs (Figure 2B) and showed no significant differences between control mice and homozygous κ-CHEB mice (mean, 7.72 ± 0.92 mg/mL vs 8.21 × 0.61 mg/mL, respectively; $P > .05$), but a significant decrease of serum κ LC in κ-CHEB/κ-del (5.33 × 1.13 mg/mL) and in homozygous κ-*Neo* mice (2.08 × 0.66 mg/mL), compared either with control ($P < .01$ and $P < .001$, respectively) or to homozygous κ-CHEB mice ($P < .001$).

Pathologic studies

In comparison with normal kidneys from control mice, samples from homozygous κ-CHEB and heterozygous κ-CHEB/κ-del mice all displayed morphologic alterations characteristic of FS. By light microscopy, intracellular rhomboid microcrystals were detected in mice proximal tubular cells by toluidine-blue staining of semithin sections (Figures 3A-C), similar to patient CHEB. However, crystal accumulation was less marked than that in patient CHEB (Figure 3D). Proximal tubular lesions were mild in heterozygous κ-CHEB/κ-del animals (Figure 3C), whereas homozygous κ-CHEB mice displayed a significant increase in the number of crystals per tubule section compared with heterozygous κ-CHEB/κ-del and

Figure 2. Efficient κ LC expression by splenocytes and serum production. (A) Flow cytometric analysis of splenocytes. Freshly isolated spleen cells were stained with anti-κ fluorescent antibodies. Representative results for each strain are indicated. Numbers indicate percentages of total lymphocytes. (B) Summary of the results obtained in κ LC serum production. Mean κ LC levels from all experiments (± SEs in italics) are indicated on top of the graph in milligrams per milliliter. Each point represents data from an individual mouse. κNH indicates homozygous κ-*Neo* mice; κC/κD, heterozygous κ-CHEB/κ-del mice; and κCH, homozygous κ-CHEB mice.

Figure 4. Transgenic mice kidneys by immunofluorescence and immunostaining. (A) Homozygous κ-CHEB mice. Immunofluorescence microscopy, polyclonal rabbit antibody against human κ-light chain, original magnification × 400. Strong peripheral staining of crystalline inclusions in the cytoplasm of proximal tubular cells. No staining was observed in glomeruli and distal tubule basement membranes and lumens. Proximal tubular cells were not stained by the anti-λ polyclonal antibody (not shown). (B) Homozygous κ-CHEB mice. Immunostaining with a rabbit polyclonal anti–mouse cathepsin B, original magnification × 1000. Heavy cytoplasmic labeling was observed in proximal tubule sections. Inset: strong peripheral staining of intracytoplasmic vacuoles containing crystalline inclusions (arrows).

Figure 3. Transgenic mice kidneys by light microscopy. (A-B) Homozygous κ-CHEB mice. Semithin sections of araldite-included samples. Toluidine blue staining, original magnification × 100 (A) and × 400 (B). Numerous crystalline inclusions in the cytoplasm of proximal tubular cells (arrows and inset). Note the absence of myeloma casts in distal tubule lumens (A), and the normal appearance of glomerular tufts and Bowman capsules (A-B). Crystalline inclusions were not observed in the initial part of proximal tubules (B, asterisk). (C) κ-CHEB/κ-del mice. Semithin sections of araldite-included samples. Toluidine blue staining, original magnification × 400. Few crystalline inclusions were present within proximal tubules (arrow). (D) Patient CHEB. Araldite-inclusion, toluidine blue staining, original magnification × 1000. Massive cytoplasmic crystalline accumulation in proximal tubular cells, with some free crystals in tubular lumen (arrow). Inclusions were not observed in glomeruli.

control mice (Figures 3A-B; Table 1). In homozygous κ-CHEB mice, the presence of numerous intracytoplasmic crystals was associated with cytoplasm atrophy. Whereas crystals were detected in a large number of proximal tubule sections, they were not equally distributed, with tubular cells filled with crystals coexisting with normal cells in the same tubule section (Figure 3B). Moreover, crystal accumulation was predominantly seen in the distal part of the proximal tubule (S3 segment), while the Bowman capsule and distal tubule were not affected (Figure 3B). Neither glomerular lesions nor myeloma casts were observed within distal tubule lumens (Figures 3A-B,4A). Crystals were not detected in bone marrow plasma cells (not shown). Proximal tubule reabsorption and crystallization of the hybrid κ-CHEB LC was demonstrated by immunohistochemistry and immunofluorescence studies, which showed that the cystoplasm of crystal-containing proximal tubular cells was brightly stained by anti-κ–specific antibodies, and not by anti-λ antibodies, with the same previously described pattern (Figure 4A).[28] Neither glomerular, vascular, or peritubular κ light-chain deposits were observed. By immunohistochemistry, cathepsin B appeared to be normally expressed in proximal tubules of homozygous κ-CHEB mice (Figure 4B). Electron microscopic analysis of proximal tubular cells of homozygous and heterozygous κ-CHEB mice showed that crystalline inclusions in proximal tubular cells were located within the endolysosomal compartment (Figure 5A-C) and displayed a regular striation of 80-Å periodicity, identical to that previously reported in patient CHEB (Figure 5D-C).[6] In homozygous κ-CHEB mice, marked crystal accumulation was associated with morphologic alterations of the proximal tubular cells, including segmental loss of the apical microvillous border and duplication of the tubular basement membrane (Figure 5A). Enlarged mitochondria were also observed, as previously reported in FS and various cases of functional tubular alterations[5,35] (Figure 5C).

Blood and urine biochemical parameters

Compared with control mice, homozygous κ-CHEB mice displayed symptoms of proximal tubular dysfunction, with significantly lower serum levels of uric acid and phosphate, higher FE of uric acid and phosphate, and increased urine excretion of CC16.
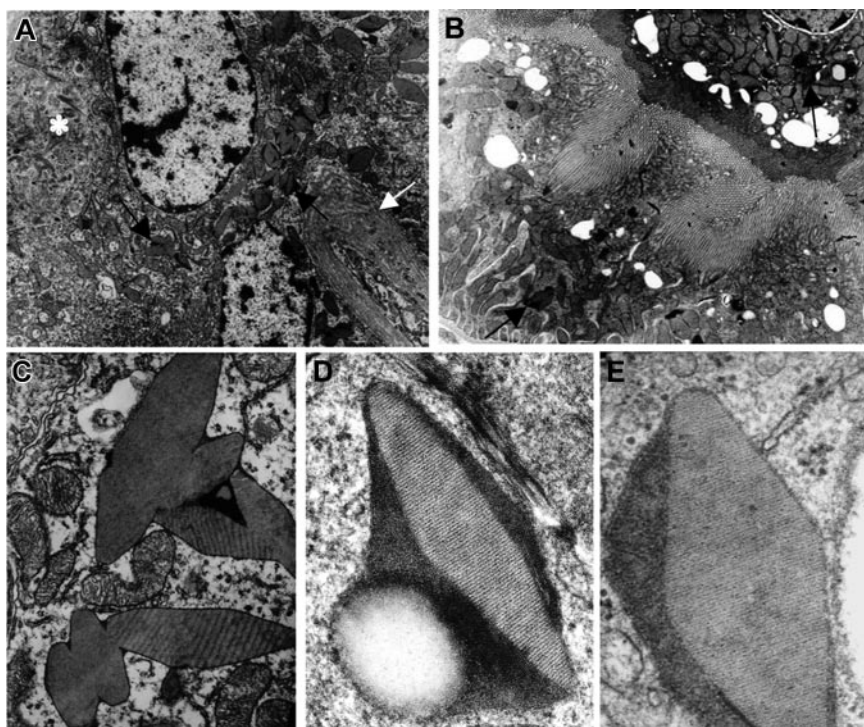
Figure 5. Electron microscopic studies. (A) Homozygous κ-CHEB mice. Electron microscopy, original magnification × 4000: numerous crystalline (arrows) and osmiophilic inclusions within the cytoplasm of proximal tubular cells. Note the alteration of apical brush border membrane (*) and duplication of the tubular basement membrane (white arrow). (B) κ-CHEB/κ-del mice. Electron microscopy, original magnification × 4000: proximal tubular cells contained few crystalline inclusions (arrows) and morphology of the brush border was preserved. (C) Homozygous κ-CHEB mice. Electron microscopy (original magnification × 12 000). Crystalline inclusions bound in a single membrane, probably related to lysosomes. Note the morphologic alterations of mitochondria. (D) Homozygous κ-CHEB mice. Electron microscopy (original magnification × 50 000) and (E) Patient CHEB. Kidney biopsy. Electron microscopy (original magnification × 80 000). Similar ultrastructural appearance of osmiophilic crystalline inclusions in patient CHEB and κ-CHEB mice, with an 80-Å periodic striation.

Serum levels of uric acid were significantly lower in κ-CHEB/κ-del mice, which also showed a trend to lower phosphatemia, higher FE of uric acid, and higher FE of phosphate, compared with control mice, but this trend did not reach statistical significance. No significant differences were observed between the 3 groups of mice in serum levels of creatinine and calcium, and in urine calcium and glucose excretion (Table 2). In comparison with controls, there was no increased aminoaciduria in the transgenic mice (data not shown).

Decreased proximal tubular lesions after conditional deletion of κ-CHEB LC

In mice injected with pI-pC in order to induce conditional deletion of the knock-in Vκ segment, PCR and flow cytometric analysis showed a rapid (but never complete) decay of the κ-CHEB LC on the surface of spleen B cells (Figure 6A-B). Consistent with this result, ELISAs made 1 month after the first injection of pI-pC showed a strong decrease (5 times) of the serum κLC level (data not shown). Two months after the pI-pC–induced deletion, mice were killed in order to allow pathologic examination of kidneys. At

this time, a significant decrease (although not a disappearance) in the density of tubular crystals inclusions was observed in homozygous κ-CHEB mice (Table 1). When the same deletion was induced in the κ-CHEB/κ-del mice expressing lower levels of the nephrotoxic LC, no more crystals were detectable in kidney proximal tubules that had returned to a normal aspect in most of the animals within 2 months. The presence of crystalline inclusions within proximal tubules before conditional deletion was checked in 2 κ-CHEB/κ-del mice by performing unilateral nephrectomy before pI-pC treatment (Figure 7).

Discussion

We have established a transgenic murine model of human FS featuring κI LC crystallization in proximal tubular cells. It has been postulated that structural peculiarities of certain LC V domains are involved in their specific nephrotoxic properties in AL amyloidosis,[11-20] nonamyloid LC deposition disease,[6,21-27] and FS.[3,5-10] The herein reported in vivo models of FS definitely show that the main nephrotoxic properties of a monoclonal FS LC are carried by the V domain and are preserved when a human V domain cloned from a patient is expressed in mice in combination with a different constant domain.

FS κ LC transgenic mice readily expressed a chimeric Vκ-CHEB/mouse Cκ LC in their peripheral splenocytes, and displayed pathologic alterations of the kidneys typical of FS with characteristic intracellular crystals, associated with enlargement of mitochondria and alterations of the apical brush-border in proximal tubule cells with heavy crystalline accumulation.

In contrast with our previous attempts to set up a model of myeloma-associated FS using transfected tumor cells that secreted a fully human FS κI chain,[28] the transgenic mice showed no obvious alteration of their general condition and were much more easily amenable to physiologic explorations than mice grafted with

Table 1. Extent of crystalline inclusions within proximal tubules

Group	Semiquantitative score of crystal formation	P
A: κ-CHEB/κ-CHEB (n)	3.1 ± 1.1 (13)	A vs B, < .01; A vs C, < .01
B: κ-CHEB/κ-del (n)	1.3 ± 0.5 (8)	A vs D, < .001; A vs E, < .001
C: controls (n)	0 (8)	B vs C, < .05; B vs D, NS
D: κ-CHEB/κ-CHEB after Vκ deletion (n)	1.1 ± 1.4 (8)	B vs E, NS; C vs D, NS; C vs E, NS
E: κ-CHEB/κ-del after Vκ deletion (n)	0.2 ± 0.2 (5)	D vs E, NS

NS indicates not significant.

Table 2. Serum and urine parameters

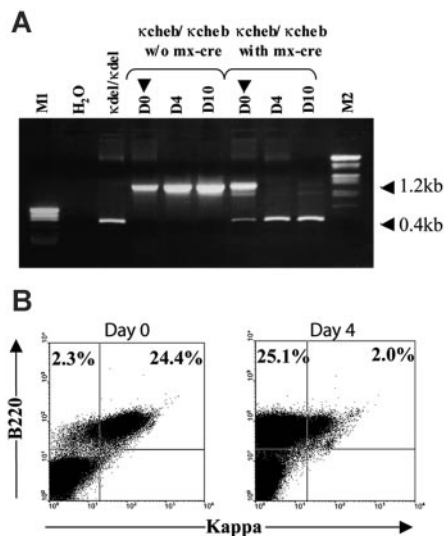| Group	A: κ-CHEB/κ-CHEB (n)	B: κ-CHEB/κ-DEL (n)	C: controls (n)	ANOVA	A vs B	A vs C	B vs C
					Unpaired _t_ test or Bonferroni multiple comparisons test		
Diuresis, μL/min	1.01 ± 0.6 (13)	ND	0.81 ± 0.47 (7)	NA	NA	0.49	NA
Serum creatinine, μM	16.6 ± 5.0 (13)	19.5 ± 4.3 (11)	17.9 ± 4.2 (10)	0.31	NS	NS	NS
Serum uric acid, μM	43.7 ± 20.1 (13)	57.0 ± 20.7 (11)	107.6 ± 52.6 (10)	0.0002	NS	< 0.001	< 0.01
FE uric acid, %	14.3 ± 11.0 (10)	10.6 ± 7.3 (11)	4.5 ± 3.5 (10)	0.03	NS	< 0.05	NS
Serum phosphate, mM	2.1 ± 0.4 (13)	2.4 ± 0.6 (11)	3.0 ± 0.4 (10)	0.003	NS	< 0.01	NS
FE phosphate, %	23.6 ± 19.1 (9)	17.9 ± 10.3 (8)	7.7 ± 3.5 (9)	0.04	NS	< 0.05	NS
Serum total calcium, mM	2.38 ± 0.06 (12)	2.47 ± 0.09 (10)	2.43 ± 0.10 (10)	0.11	NS	NS	NS
Urine calcium/creatinine, mM/mM	0.74 ± 0.32 (13)	0.62 ± 0.39 (11)	0.81 ± 0.30 (10)	0.42	NS	NS	NS
FE calcium, %	0.49 ± 0.21 (13)	0.41 ± 0.20 (10)	0.58 ± 0.19 (10)	0.2	NS	NS	NS
Urine glucose/creatinine, mM/mM	0.15 ± 0.1 (12)	0.15 ± 0.1 (11)	0.09 ± 0.08 (9)	0.64	NS	NS	NS
Urine CC16/creatinine, μg/g	756 ± 1496 (13)	ND	75 ± 30 (7)	NA	NA	0.008	NA

NS indicates not significant; FE, fractional excretion; ND, not done; and NA, not applicable.

tumors. In the latter, the poor general condition and nonspecific lesions resulting from rapid tumor growth prevented in vivo biochemical studies. In transgenic mice, we were able to carry out serum and urine electrolyte determinations, and to show that the transgenic homozygous animals had significant impairment of uric acid, phosphate, and CC16 tubular reabsorption, 3 cardinal features of FS.[33,34] Strikingly, both proximal tubular morphologic lesions and impairment of reabsorption function appeared to be related to the rate of production of the pathogenic Vκ LC. This could account for the phenotypic differences between patient CHEB and transgenic mice, the latter showing less crystalline accumulation within proximal tubules, milder morphologic cellular alterations, and no significant glucosuria or aminoaciduria.
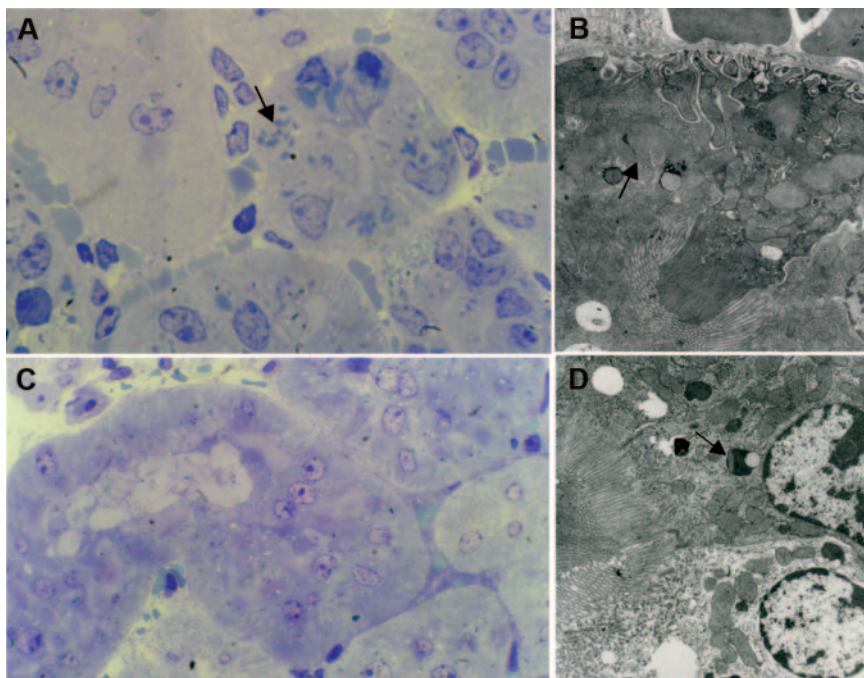
Although not solely involved in FS, it is likely that the germinally encoded framework Vκ _O2/O12_ gene sequence carries

Figure 6. Decay of κCHEB LC upon conditional deletion by pI-pC. (A) PCR analysis of VκJκ _CHEB_ deletion after pI-pC injection. PCR was performed on splenocytes DNA of killed mice at days 0, 4, and 10 after pI-pC injection. The 1.2-kb and 0.4-kb bands correspond to the undeleted and the deleted VκJκ gene, respectively, using 5′Jκ and 3′Jκ primers indicated in Figure 1. M1 indicates pBS _Hpa_II ladder; M2, λ HIII/_Eco_RI ladder. (B) Flow cytometric analysis of B220-positive splenocytes at days 0 and 4 after pI-pC injection. Freshly isolated spleen cells were stained with anti-B220 and anti-κ fluorescent antibodies. Percentages of κ-positive and κ-negative B220-positive cells are indicated.

by itself a propensity to induce proximal tubule dysfunction and to promote LC crystallization, provided additional modifications of the V sequence are created by the somatic hypermutation process. FS LCs derived from the _O2/O12_ germ-line gene are nearly always characterized by the presence of unusual hydrophobic or nonpolar residues in the CDR-L1 loop at position 30 and, at variance with κ LCs responsible for myeloma cast nephropathy, show a remarkable resistance to proteolytic digestion by trypsin and by cathepsin B, the main lysosomal enzyme in renal proximal tubule. These unique properties have been proposed to be involved in the accumulation of crystals within the endolysosomal compartment of proximal tubules in FS, leading to impairment of the proximal tubular-cell function.[5-8] We previously demonstrated that the concomitant presence of hydrophobic amino-acid replacements at positions 30 and 94 were needed in order for the CHEB LC to display its property to assemble into crystals.[28] By engineering mice in which B cells spontaneously produce LC with a V domain similar to that expressed in a patient with myeloma-associated FS, including the Ser → Ala +30 and Thr → Ile +94 replacements, we show that even when associated with an heterologous murine C domain, the CHEB V domain may develop its nephrotoxic properties. Taken together, our data directly demonstrate that sequence peculiarities of the κ chain V domain are implicated in the process of LC crystallization that occurs in most cases of myeloma-associated FS.

This transgenic model provides ideally suited material to explore the mechanisms by which nephrotoxic LCs disturb the complex reabsorptive functions of the proximal tubule. Recent studies have demonstrated that some monoclonal VκI LCs encoded by the _O8/O18_ germ-line gene, as well as VκIII LCs, may induce full-blown FS or incomplete proximal tubular dysfunction, despite their normal sensitivity to proteolysis and the absence of crystal accumulation within the proximal tubules.[8,10,36] These data strongly suggest that monoclonal LCs in FS might interfere with proximal tubule reabsorption function through direct toxic effects. Circulating free LCs, after being freely filtered by the glomerulus, are reabsorbed in the proximal tubule by a mechanism of endocytosis involving LC binding to the low-affinity, high-capacity multiligand receptors cubilin and megalin, located in the intermicrovillar areas of the apical brush border. After fusion of endosomes with primary lysosomes, LCs are degraded by lysosomal proteases, mainly cathepsin B, into amino acids that are recycled through the

Figure 7. Effect of κCHEB LC conditional deletion on renal morphology. (A-B) κ-CHEB/κ-del mouse, left nephrectomy, performed before pI-pC–induced VκJκ *CHEB* deletion. (A) Light microscopy, araldite inclusion, toluidine blue staining, oil immersion (original magnification × 1000). (B) Electron microscopy (original magnification × 5000). Numerous crystalline inclusions within the cytoplasm of proximal tubular cells (arrows). (C-D). Same κ-CHEB/κ-del mouse, right nephrectomy, performed 2 months after pI-pC–induced VκJκ *CHEB* deletion. (C) Light microscopy, araldite inclusion, toluidine blue staining, oil immersion (original magnification × 1000). No more crystalline inclusions were observed in proximal tubular cells. By electron microscopy (panel D, original magnification × 5000), only few and small crystals were detected in phagolysosomes of proximal tubular cells (arrow).

basolateral membrane.[37] Pioneer studies by Sanders et al have established that monoclonal LCs, purified from the urine of myeloma patients with renal failure (and no evidence of associated FS), had specific nephrotoxic properties, probably related to distinct physicochemical characteristics. When perfused in rat nephron in vivo, some LCs precipitated in the distal tubules, while others induced morphologic damage of the proximal tubule epithelium, with focal loss of the microvillous border, vacuolation, and desquamation of cell fragments. Immunolabeling studies showed that LCs accumulated in the endolysosomal system, activated and disrupted lysosomes. Proximal tubule function was altered, as demonstrated by reduced absorption of water, chloride, and glucose.[38,39] In further in vitro studies, purified human monoclonal LCs were shown to induce inhibition of brush-border membrane sodium cotransporters,[40,41] and to decrease basolateral Na-K-ATPase expression and activity.[42] Similar mechanisms could be involved in the pathogenesis of monoclonal LC–associated FS. FS monoclonal LCs could also impair oxidative phosphorylation and mitochondrial energy supply[5] and interfere with the recycling of specific transporters to the apical membrane of the proximal tubular cells by impairing early endosomal and lysosomal acidifica-

tion.[34,43] In that regard, our present model should be of great help for identifying the cellular targets of reabsorbed monoclonal nephrotoxic light chains and for testing drugs potentially counteracting these effects.

As human FS is generally associated with monoclonal gammopathy in the absence of overt multiple myeloma, chemotherapy is considered to be of little benefit, despite progression to end-stage renal disease in many patients.[5,44] However, the reversibility of proximal tubule morphologic alterations when deletion of the knock-in V gene was induced into mice suggests that in patients with FS, reducing the tumor mass and decreasing production of the nephrotoxic monoclonal LCs would not only stop the accumulation of deposits but also promote their regression.

Acknowledgments

References

1. Preud'homme JL, Aucouturier P, Touchard G, et al. Monoclonal immunoglobulin deposition disease: a review of immunoglobulin chain alterations. Int J Immunopharmacol. 1994;16:425-431.

2. Solomon A, Weiss DT. A perspective of plasma cell dyscrasias: clinical implications of monoclonal light chains in renal disease. In: Minetti L, d'Amico G, Ponticelli C, eds. The Kidney in Plasma Cell Dyscrasias. Dordrecht, Netherlands; Kluwen Academic Publishers, 1988:3-10.

3. Pirani C, Silva F, d'Agati V, Chander P, Striker L. Renal lesions in plasma cell dyscrasias: ultrastructural observations. Am J Kidney Dis. 1987; 10:208-221.

4. Sanders PW, Booker BB, Bishop JB, Cheung HC. Mechanisms of intranephronal proteinaceous

cast formation by low molecular weight proteins. J Clin Invest. 1990;85: 570-576.

5. Messiaen T, Deret S, Mougenot B, et al. Adult Fanconi syndrome secondary to light chain gammopathy: clinicopathologic heterogeneity and unusual features in 11 patients. Medicine (Baltimore). 2000;79:135-154.

6. Aucouturier P, Bauwens M, Khamlichi AA, et al. Monoclonal Ig L chain and L chain V domain fragment crystallisation in myeloma-associated Fanconi's syndrome. J Immunol. 1993;150:3561-3568.

7. Leboulleux M, Lelongt B, Mougenot B, et al. Protease resistance and binding of Ig light chains in myeloma-associated tubulopathies. Kidney Int. 1995;48:72-79.

8. Deret S, Denoroy L, Lamartine M, et al. Kappa light chain-associated Fanconi's syndrome:

molecular analysis of monoclonal immunoglobulin light chains from patients with and without intracellular crystals. Protein Eng. 1999;12:363-369.

9. Rocca A, Khamlichi AA, Touchard G, et al. Light chain V region gene usage restriction and peculiarities in myeloma-associated Fanconi's syndrome. J Immunol. 1995;155:3245-3252.

10. Decourt C, Bridoux F, Touchard G, Cogné M. A monoclonal VκI light chain responsible for incomplete proximal tubulopathy. Am J Kidney Dis. 2003;41:497-504.

11. Solomon A, Frangione B, Francklin EC. Bence Jones proteins and light chains of immunoglobulins: preferential association of the VλVI subgroup of human light chains with amyloidosis AL(1). J Clin Invest. 1982;70:453-460.

12. Eulitz M, Linke R. Amyloid fibrils derived from V-region together with C-region fragments from a

lambda II-immunoglobulin light chain (HAR). Biol Chem Hoppe Seyler. 1985;366:907-915.

13. Toft KG, Sletten K, Husby G. The amino-acid sequence of the variable region of a carbohydrate-containing amyloid fibril protein EPS (immunoglobulin light chain, type lambda). Biol Chem Hoppe Seyler. 1985;366:617-625.

14. Tveteraas T, Sletten K, Westermark P. The amino acid sequence of a carbohydrate-containing immunoglobulin-light-chain-type amyloid-fibril protein. Biochem J. 1985;232:183-190.

15. Dwulet FE, Strako K, Benson MD. Amino acid sequence of a lambda VI primary (AL) amyloid protein (WLT). Scand J Immunol. 1985;22:653-660.

16. Dwulet FE, O'Connor TP, Benson MD. Polymorphism in a kappa I primary (AL) amyloid protein (BAN). Mol Immunol. 1986;23:73-78.

17. Holm E, Sletten K, Husby G. Structural studies of a carbohydrate-containing immunoglobulin lambda-light-chain amyloid-fibril protein (AL) of variable subgroup III. Biochem J. 1986;239:545-551.

18. Benson MD, Dwulet FE, Madura D, Wheeler G. Amyloidosis related to a lambda IV immunoglobulin light chain protein. Scand J Immunol. 1989;29:175-179.

19. Liepnieks JJ, Dwulet FE, Benson MD. Amino acid sequence of a kappa I primary (AL) amyloid protein (AND). Mol Immunol. 1990;27:481-485.

20. Aucouturier P, Khamlichi AA, Preud'homme JL, Bauwens M, Touchard G, Cogné M. Complementary DNA sequence of human amyloidogenic immunoglobulin light-chain precursors. Biochem J. 1992;285:149-152.

21. Cogné M, Preud'homme JL, Bauwens M, Touchard G, Aucouturier P. Structure of a monoclonal kappa chain of the VκIV subgroup in the kidney and plasma cells in light chain deposition disease. J Clin Invest. 1991;87:2186-2190.

22. Bellotti V, Stoppini M, Merlini G, et al. Amino acid sequence of k Sci, the Bence Jones protein isolated from a patient with light chain deposition disease. Biochem Biophys Acta. 1991;1097:177-182.

23. Khamlichi AA, Aucouturier P, Silvain C, et al. Primary structure of a monoclonal κ chain in myeloma with light chain deposition disease. Clin Exp Immunol. 1992;87:122-126.

24. Rocca A, Khamlichi AA, Aucouturier P, et al. Primary structure of a variable region of the VκI subgroup (ISE) in light chain deposition disease. Clin Exp Immunol. 1993;91:506-509.

25. Decourt C, Cogné M, Rocca A. Structural peculiarities of a truncated VκIII immunoglobulin light chain in myeloma with light chain deposition disease. Clin Exp Immunol. 1996;106:357-361.

26. Decourt C, Touchard G, Preud'homme JL, et al. Complete primary sequences of two λ immunoglobulin light chains in myelomas with non-amyloid (Randall type) light chain deposition disease. Am J Pathol. 1998;153:313-318.

27. Khamlichi AA, Rocca A, Touchard G, Aucouturier P, Preud'homme JL, Cogné M. Role of light chain variable region in myeloma with light chain deposition disease: evidence from an experimental model. Blood. 1995;86:3655-3659.

28. Decourt C, Rocca A, Bridoux F, et al. Mutational analysis in murine models for myeloma associated Fanconi's syndrome or cast myeloma nephropathy. Blood. 1999;94:3559-3566.

29. Saïki RK, Scharf S, Fallona F. Enzymatic amplification of β-globin genomic sequences and restriction site analysis for diagnosis of sickle cell anemia. Science. 1985;230:1350-1354.

30. Sanger F, Nicklen S, Coulson AR. DNA sequencing with chain-terminating inhibitors. Proc Natl Acad Sci U S A. 1977;74:5463-5467.

31. Kuhn R, Schwenk F, Aguet M, Rajewsky K. Inducible gene targeting in mice. Science. 1995;269:1427-1429.

32. Ma LJ, Fogo AB. Model of robust induction of glomerulosclerosis in mice: importance of genetic background. Kidney Int. 2003;64:350-355.

33. Bernard AM, Thielemans NO, Lauwerys RR. Urinary protein 1 or Clara cell protein: a new sensitive marker of proximal tubular dysfunction. Kidney Int. 1994;47:34-37.

34. Wang SS, Devuyst O, Courtoy PJ, et al. Mice lacking renal chloride channel, CLC-5, are a model for Dent's disease, a nephrolithiasis disorder associated with defective receptor-mediated endocytosis. Hum Mol Genet. 2000;9:2937-2945.

35. Niaudet P, Rotig A. Renal involvement in mitochondrial cytopathies. Pediatr Nephrol. 1996;10:368-373.

36. Bridoux F, Sirac C, Hugue V, et al. Fanconi's syndrome induced by a monoclonal Vkappa3 light chain in Waldenstrom's macroglobulinemia. Am J Kidney Dis. 2005;45:749-757.

37. Klassen RB, Allen PL, Batuman V, Crenshaw K, Hammond TG. Light chains are a ligand for megalin. J Appl Physiol. 2005;98:257-263.

38. Sanders PW, Herrera GA, Galla JH. Human Bence Jones protein toxicity in rat proximal tubule epithelium in vivo. Kidney Int. 1987;32:851-861.

39. Sanders PW, Herrera GA, Chen A, Booker BB, Galla JH. Differential nephrotoxicity of low molecular weight proteins in the perfused rat nephron in vivo. J Clin Invest. 1988;82:2086-2096.

40. Batuman V, Sastrasinh M, Sastrasinh S. Light chain effects on alanine and glucose uptake by renal brush border membranes. Kidney Int. 1986;30:662-665.

41. Batuman V, Guan S, O'Donovan R, Puschett JB. Effect of myeloma light chains on phosphate and glucose transport in renal proximal tubular cells. Ren Physiol Biochem. 1994;17:294-300.

42. Guan S, El-Dahr S, Dipp S, Batuman V. Inibition of Na-K-ATPase activity and gene expression by a myeloma light chain in proximal tubule cells. J Investig Med. 1999;47:496-501.

43. Nicastri AL, Brandao de Almeida Prado MJ, Sesso A, Brandao de Almeida Prado EB. Defective proximal tubule lysosomal acidification by Bence Jones proteins: an immunoelectron microscopy study. Exp Nephrol. 1998;6:514-521.

44. Ma CX, Lacy MQ, Rompala JF, et al. Acquired Fanconi syndrome is an indolent disorder in the absence of overt multiple myeloma. Blood. 2004;104:40-42.